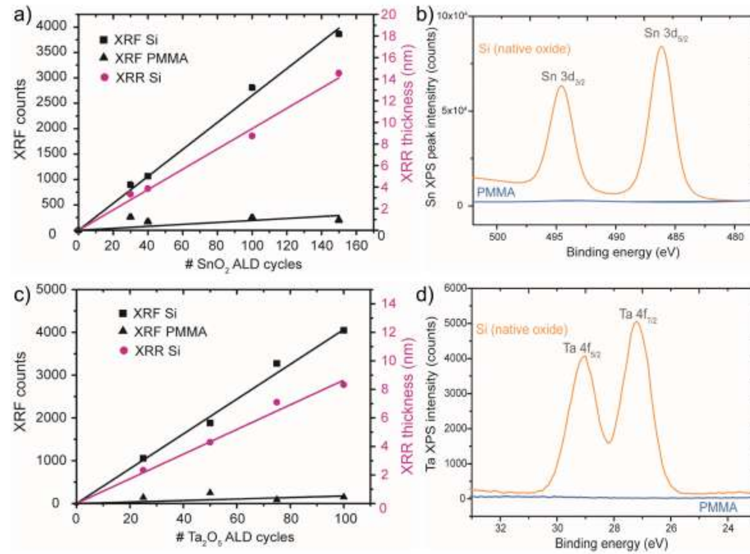


Figure 1: Thickness measurements of (a) ALD $SnO_2$ deposited on blanket Si and PMMA substrates and (c) ALD $Ta_2O_5$ deposited on blanket Si and PMMA substrates. XPS measurements of (b) 80 cycles of ALD $SnO_2$ on blanket Si and PMMA substrates and (d) 80 cycles of ALD $Ta_2O_5$ on blanket Si and PMMA substrates. The results confirm the selectivity of the ALD processes, demonstrating linear ALD growth on Si with negligible growth on PMMA up to 100 cycles.

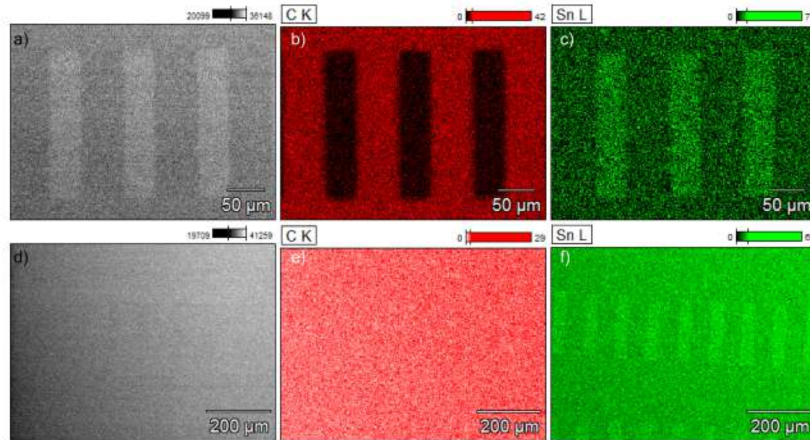


Figure 2: EDS mapping scans of ALD $SnO_2$ films deposited on a PMMA patterned substrate: (a) Pattern image and elemental maps for (b) C and (c) Sn for as-deposited films on the pattern. (d) Pattern image and elemental maps for (e) C and (f) Sn after removing the template PMMA layer using $O_2$ plasma. The images demonstrate that PMMA can inhibit the growth of ALD $SnO_2$ and the compatibility of this process with AS-ALD.

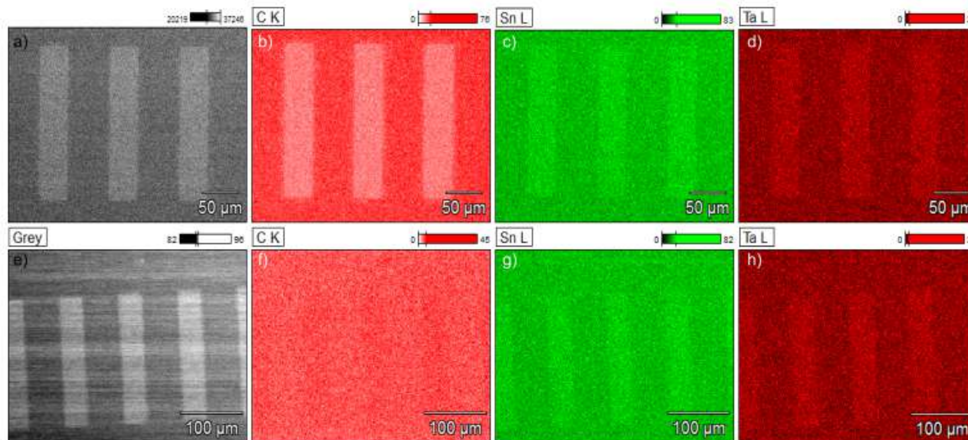


Figure 3: EDS mapping scans of bilayer ALD $SnO_2$-$Ta_2O_5$ films deposited on a PMMA patterned substrate: (a) Pattern image, elemental maps for (b) C, (c) Sn and (d) Ta for as-deposited films on the pattern. (e) Pattern image, elemental maps for (f) C, (g) Sn and (h) Ta after removing the template PMMA layer using $O_2$ plasma. The results indicate that PMMA can inhibit the growth of both ALD $SnO_2$ and $Ta_2O_5$ and the compatibility of PMMA with AS-ALD using two separate dimethylamide precursors.